QCD and spin effects in black hole airshowers

Marco Cavaglià* and Arunava Roy†
Department of Physics and Astronomy, University of Mississippi, University, MS 38677-1848, USA

(Dated: February 8, 2022)

In models with large extra dimensions, black holes may be produced in high-energy particle collisions. We revisit the physics of black hole formation in extensive airshowers from ultrahigh-energy cosmic rays, focusing on collisional QCD and black hole emissivity effects. New results for rotating black holes are presented. Monte Carlo simulations show that QCD effects and black hole spin produce no observable signatures in airshowers. These results further confirm that the main characteristics of black hole-induced airshowers do not depend on the fine details of micro black hole models.

PACS numbers: 04.50.+h, 04.70.Dy, 96.50.Sd, 13.85.Tp

arXiv:0707.0274v1 [hep-ph] 2 Jul 2007

I. INTRODUCTION

In an effort to unify gravity with the other fundamental forces, we are faced with the hierarchy problem. The fundamental scale of gravity is about 17 orders of magnitude higher than the TeV scale, where electromagnetic and weak forces unify. The hierarchy problem may be solved by the introduction of large extra dimensions [1]. In this model, the Planck scale $M_{\rm Pl}$ is related to the fundamental scale of gravity $M_\star \sim 1$ TeV by the relation $M_{\rm Pl}^2 \sim V_n M_\star^{n+2}$, where V_n is the volume of the extra n-dimensional space. Gravity is a strong force in the higher-dimensional spacetime but appears weak to a four-dimensional observer due to its "leakage" in the extra dimensions. Gravitons may propagate in all dimensions (bulk). Compatibility with known sub-TeV physics restricts the propagation of all Standard Model (SM) fields to three spatial dimensions (brane).

One of the effects of the increased strength of gravity would be the production of TeV-scale Black Holes (BHs) in high-energy particle collisions [2]. Micro BHs could be produced in man-made particle colliders, e.g. the Large Hadron Collider [3, 4, 5], or naturally in Earth's atmosphere by Ultra High Energy Cosmic Rays (UHECRs) interacting with air nucleons [6, 7, 8, 9]. (For reviews, see Refs. [10].) Once formed, these BHs would immediately decay through loss of excess multipole moments (balding phase), Hawking emission [11] (evaporation phase) and final n-body decay or remnant production (Planck phase). SM fields may be originated in each of these stages, providing a means to detect the BHs. For atmospheric events, the visible imprint would be an extensive airshower initiated by these SM quanta.

The characteristics of BH-induced airshowers can be investigated with Monte Carlo techniques. A Monte Carlo code for BH formation and airshower generation is GROKE [12]. GROKE simulation of BH events proceeds in three stages. First, the BH is formed by the collision of an UHE neutrino and an air nucleon parton. Some of the Center-of-Mass (CM) energy is lost in the process (about 40% for head on collisions, monotonically increasing with the impact parameter [13, 14]). SM unstable particles from the BH decay and the nucleon remnant are hadronized using a high-energy physics program for event generation (PYTHIA) [15]. PYTHIA's output is then injected into a simulator of extensive airshowers (AIRES) [16]. Simulations show that BH airshowers generally rise faster, have broader peak and higher variation in the total energy than SM airshowers because of the "democratic" nature of BH decay. BH events are also characterized by a larger muonic content at the ground compared to SM events due to the dominant hadronic channel in the BH evaporation phase. A complete discussion of BH signatures can be found in Refs. [8, 12].

BH searches require the identification of observational signatures that do not depend on the fine details of the model. This can be achieved by improving the theoretical description of the event and then testing the stability of the airshower characteristics against these theoretical refinements. Previous investigations [8, 12] neglected or approximated various aspects of the physics of BH formation and decay such as QCD effects, BH spin and particle emissivities. QCD effects in the fragmentation process may lead to changes in the amount of visible energy deposited

*Electronic address: cavaglia@olemiss.edu
†Electronic address: arunav@olemiss.edu

in the airshower by the nucleon remnant. Changes in particle emissivities due to spacetime dimensionality or BH rotation may affect rapidity, peak variation and muon content of airshowers. The aim of this paper is to check the stability of BH airshowers characteristics when these effects are included. The result of our investigation is that inclusion of collisional QCD effects, changes in particle emissivity and BH rotation do not significantly affect the BH airshower development: Observational signatures of BH events are robust. Natural units are used throughout the paper with $M_* = 1$.

II. QCD AND EMISSIVITY EFFECTS

QCD effects in airshower generation and development include initial- and final-state radiation, fragmentation, and the hadronization process of nucleon remnant and unstable quanta. Since PYTHIA is designed to handle initial- and final-state radiation, multiple scattering, beam remnant and hadronization, these effects can be investigated by modifying the GROKE code [12] to include the BH event as a PYTHIA external process.

The BH airshower is initiated by the decay products of the BH, the nucleon remnant and jets from initial- and final-state radiation. The colliding parton is taken from the Parton Distribution Functions at a very high energy scale ($\gtrsim$ TeV). This implies that it typically emits quite hard initial-state radiation before it collides to form a black hole, resulting in additional jets. In addition, the nucleon remnant undergoes soft and semi-hard multiple scatterings which will contribute to the airshower. Previous investigations of BH airshowers did also not take into account color conservation. However, the nucleon remnant is color connected to the BH decay products; the color flow will also hadronize into more jets. In our investigation, color flow is implemented in the $N_C \to \infty$ limit of QCD [15].

Total multiplicity (N) and multiplicity per species (N_i) of the BH decay are essential to determine the airshower characteristics. Earlier studies [8, 12] used approximated thermally-averaged emissivities (graybody factors) for the evaporation phase. Recently, exact graybody factors for higher-dimensional nonrotating BHs were calculated in Ref. [17]. Changes in greybody factors are specially relevant for higher-dimensional spacetimes, where graviton emission is highly enhanced. These results are implemented in GROKE following Ref. [5]. The total multiplicity in the evaporation phase is

$$N = \frac{(n+1)S}{4\pi} \frac{\sum_i c_i \mathcal{R}_i \Gamma_{\mathcal{R}_i}}{\sum_j c_j \mathcal{P}_j \Gamma_{\mathcal{P}_j}}, \tag{1}$$

where S is the initial entropy of the BH, c_i are the degrees of freedom of the i-th species, and $\Gamma_{\mathcal{P}_i}$ and $\Gamma_{\mathcal{R}_i}$ are the fraction of radiated power and the emission rate per degree of freedom, respectively. The decay multiplicity per species is

$$N_i = N \frac{c_i \mathcal{R}_i \Gamma_{\mathcal{R}_i}}{\sum_j c_j \mathcal{R}_j \Gamma_{\mathcal{R}_j}}. \tag{2}$$

The use of exact greybody factors (nonrotating case) leads to a slight reduction in the output of visible energy and an enhancement of graviton multiplicity in the evaporation phase compared to previous studies. These effects are generally of order ~ 1 or less.

QCD and emissivity effects on the BH airshower development can be determined by looking at the longitudinal development of the e^+e^- component of the airshower and the muonic content at ground. The left panel of Fig. 1 compares 50 BH airshowers with and without QCD and emissivity effects (primary neutrino energy $E_\nu = 10^{19}$ eV, ten spacetime dimensions). The average depth of the airshower maxima X_m is not significantly affected by the inclusion of initial- and final-state radiation, color conservation and exact emissivities. This can be qualitatively explained by looking at the energy distribution of the BH airshower initiators after the hadronization and fragmentation process. PYTHIA's output shows that the additional jets from initial- and final state radiation are generally too soft to affect the airshower development, which is mainly determined from the evolution of the nucleon remnant and the hard hadronic jets from the BH evaporation. The implementation of color conservation slightly changes the details of the hadronization process of previous studies. However, the main characteristics of the airshower depend on the hadronic nature of the event rather than the details of the fragmentation. Differences in the fragmentation model are washed out by uncertainties in the airshower development. A similar qualitative explanation applies to the emissivity effects. Even for massive BH events, when quanta from the evaporation phase dominate over quanta from the Planck phase and the nucleon remnant, changes due to the use of exact greybody factors are too small to produce an observable effect in the airshower profile. Identical conclusions are reached by comparing the number of muons at various depths vs. the number of e^+e^- pairs at the airshower maximum (right panel of Fig. 1).

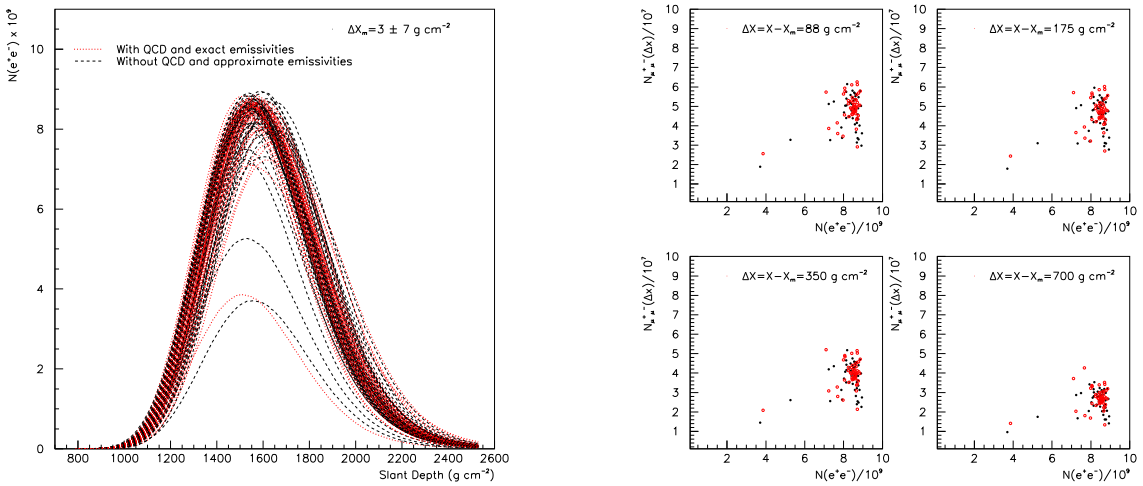


FIG. 1: Left panel: Number of e^+e^- pairs vs. slant depth for the longitudinal development of 50 ten-dimensional BH airshowers. The neutrino primary energy is $E_\nu = 10^{19}$ TeV, the altitude of the first interaction depth is 10 km (slanth depth 780 g cm^{-2}) and the zenith angle is 70°. BH airshowers without (with) QCD and emissivity effects are shown by black dashed (red dotted) curves. Right panel: Number of $\mu^+\mu^-$ pairs at various atmospheric depths $X_m + \Delta X$ vs. the number of e^+e^- at the shower maximum. BH airshowers without (with) QCD and emissivity effects are shown by black filled (red empty) circles. The observation depth increases from left to right and top to bottom.

III. ROTATING BLACK HOLES

Up to now, simulations of BH airshowers have focused on Schwarzschild BHs [8, 9, 12]. However, BHs created in collisions with nonzero impact parameter are expected to be spinning. Since the evaporation process depends on the BH angular momentum, airshowers initiated by spinning BHs could be significantly different from airshowers initiated by Schwarzschild BHs. If the graviton emissivity for rotating BHs is much higher than the emissivity of SM particles, only gravitons will be emitted, making the BH undetectable. Although particle emissivities for higher-dimensional rotating BHs are not fully known [18], the effects of rotation in the evaporation phase can be estimated from results in four dimensions and for higher-dimensional nonrotating BHs.

In four dimensions, the evaporation phase of a spinning BH with large angular momentum is dominated by gravitons [19]. The emissivity of spin-2 fields increases by a factor $\sim 10^2 - 10^3$ more than the emissivity of lower spin particles when the angular momentum increases from $J = 0$ to the maximum value $J_{max} = M^2$, where M is the mass of the BH. For a random distribution of BH spins, the average increase in graviton emissivity is ~ 10 more than the other fields. Graviton emission also increases with the number of dimensions due to a higher number of spin-2 helicity states. This has been shown quantitatively in Ref. [17] for nonrotating BHs. The graviton-to-SM emission ratio increases from 1:10^3 in four dimensions to 1:4 in eleven dimensions.

The results above suggest a larger graviton greybody factor for higher-dimensional, spinning BHs. The increase in graviton emissivity is specially relevant for ultra-spinning BHs. If most of the BHs produced in UHECR collisions are low-spinning, graviton emission is likely to increase on average by one order of magnitude more than the other fields. If most of the BHs are ultra-spinning, graviton emission could be enhanced by several orders of magnitude. It is thus crucial to determine the distribution of BH spins in airshowers. To this purpose, let us define the parameter a [3]:

$$a = \frac{D-2}{2}\frac{J}{MR}\,, \tag{3}$$

where D is the number of dimensions and R is the BH radius. The radius of the BH is related to the mass and angular momentum by the relation [20]

$$R = \frac{1}{\sqrt{\pi}}\left[\frac{8M}{1+a^2}\frac{\Gamma\left(\frac{D-1}{2}\right)}{D-2}\right]^{1/(D-3)}\,. \tag{4}$$

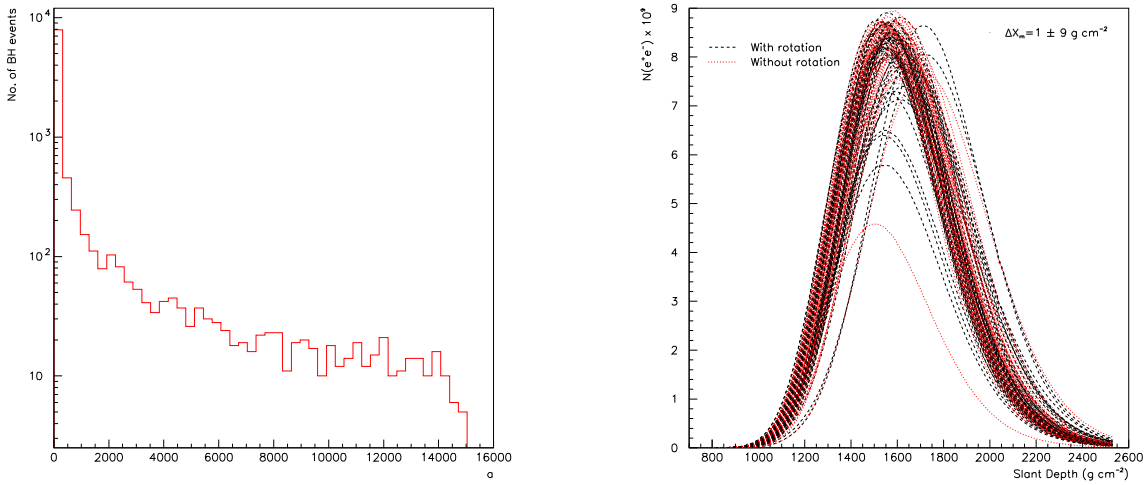


FIG. 2: Left Panel: Histogram of the number of events vs. a for the decay of a ten-dimensional rotating BH. Right Panel: Shower profiles for both rotating and nonrotating BHs. The black dashed (red dotted) curves denote rotating (nonrotating) BH events.

We consider the model of Ref. [14] for BH formation. The colliding particles are described by boosted Schwarzchild solutions at fixed energy (Aichelburg-Sexl shock waves) [21]. The BH is formed when the two waves are superposed to form a trapped surface. The mass of the BH is related to the CM energy of the colliding particles, E_{cm}, by $M = E_{cm}y$, where y depends on the impact parameter b of the collision. The ratio J/M in Eq. (3) is

$$\frac{J}{M} = \frac{xr_0}{2y}, \tag{5}$$

where $x = b/r_0$ is the impact parameter normalized to $r_0 = (4\pi E_{cm}/\Omega_{D-3})^{1/(D-3)}$ and Ω_{D-3} is the area of the unit sphere in $D-3$ dimensions. The parameter a is the solution of the polynomial equation

$$a^{D-3} = C\frac{1+a^2}{y}\left(\frac{x}{y}\right)^{D-3}, \tag{6}$$

where

$$C = \sqrt{\pi}\left(\frac{D-2}{4}\right)^{D-2}\frac{\Gamma(\frac{D-2}{2})}{\Gamma(\frac{D-1}{2})}. \tag{7}$$

The left panel of Fig. 2 gives the distribution of a for 10,000 events in ten dimensions. Most of the BH are formed with small angular momentum. This is somehow expected because the BH production cross section is reduced by a factor of $(1+a^2)^{-2/(D-3)}$ compared to the nonrotating case [7, 22]. According to the discussion above, the increase in graviton emissivity relative to lower-spin fields can be estimated to be about one order of magnitude compared the nonrotating case.

Simulations for spinning BHs with $\Gamma_{\mathcal{R}_2} \sim \Gamma_{\mathcal{P}_2} = 10\times(\text{nonrotating}\,\Gamma_{\mathcal{R}_2}, \Gamma_{\mathcal{P}_2})$ show that most of the emission is in the form of gravitons. However, the number of observable secondaries for both rotating and nonrotating BH airshowers is stable and the difference in the profiles is statistically not significant (right panel of Fig. 2). In a typical event, the bulk of the collisional CM energy is carried by the nucleon remnant. Therefore, changes in particle emissivities have generally minor effects on the airshower characteristics. Rare events ($\lesssim 10$ %) are characterized by a very low energy output. This happens when the BH carries most of the collisional energy. In these cases, the nucleon remnant does not shower and the visible energy is highly reduced by the increased graviton emission from the BH.

IV. CONCLUSIONS

This paper focused on two aspects of BH airshowers which had been neglected in previous studies: QCD and BH spin effects. The inclusion of these effects is important to check the stability of the airshower profiles and provide a more accurate template for observational searches. Event simulations based on the GROKE Monte Carlo show no change in the overall characteristics of the airshowers. Effects due to color conservation, initial- and final-state radiation, and different fragmentation models are washed out during the airshower development. BH spin effects in the airshower development are estimated to be typically small for two reasons: (i) most BHs are formed with low angular momentum and (ii) most of the CM energy is carried by the nucleon remnant. It should be stressed, however, that a conclusive statement on this issue requires the knowledge of the exact spinning BH greybody factors for all fields in higher-dimensions.

Acknowledgements

The authors thank Vitor Cardoso for many useful discussions and suggestions. This work was supported (in part) by U.S. DoE contract DE-FG05-91ER40622.

[1] N. Arkani-Hamed, S. Dimopoulos and G. R. Dvali, Phys. Lett. B **429**, 263 (1998) [arXiv:hep-ph/9803315];
I. Antoniadis, N. Arkani-Hamed, S. Dimopoulos and G. R. Dvali, Phys. Lett. B **436**, 257 (1998) [arXiv:hep-ph/9804398];
N. Arkani-Hamed, S. Dimopoulos and G. R. Dvali, Phys. Rev. D **59**, 086004 (1999) [arXiv:hep-ph/9807344].
[2] T. Banks and W. Fischler, *A model for high energy scattering in quantum gravity*, arXiv:hep-th/9906038.
[3] S. B. Giddings and S. D. Thomas, Phys. Rev. D **65**, 056010 (2002) [arXiv:hep-ph/0106219].
[4] S. Dimopoulos and G. Landsberg, Phys. Rev. Lett. **87**, 161602 (2001) [arXiv:hep-ph/0106295];
E. J. Ahn, M. Cavaglià and A. V. Olinto, Astropart. Phys. **22**, 377 (2005) [arXiv:hep-ph/0312249].
[5] M. Cavaglià, R. Godang, L. Cremaldi and D. Summers, *Catfish: A Monte Carlo simulator for black holes at the LHC*, arXiv:hep-ph/0609001.
[6] J. L. Feng and A. D. Shapere, Phys. Rev. Lett. **88**, 021303 (2002) [arXiv:hep-ph/0109106];
A. Ringwald and H. Tu, Phys. Lett. B **525**, 135 (2002) [arXiv:hep-ph/0111042];
J. Alvarez-Muniz, J. L. Feng, F. Halzen, T. Han and D. Hooper, Phys. Rev. D **65**, 124015 (2002) [arXiv:hep-ph/0202081];
J. I. Illana, M. Masip and D. Meloni, Phys. Rev. D **72**, 024003 (2005) [arXiv:hep-ph/0504234];
V. Cardoso, M. C. Espirito Santo, M. Paulos, M. Pimenta and B. Tome, Astropart. Phys. **22**, 399 (2005) [arXiv:hep-ph/0405056].
[7] L. A. Anchordoqui, J. L. Feng, H. Goldberg and A. D. Shapere, Phys. Rev. D **65**, 124027 (2002) [arXiv:hep-ph/0112247].
[8] E. J. Ahn, M. Ave, M. Cavaglià and A. V. Olinto, Phys. Rev. D **68**, 043004 (2003) [arXiv:hep-ph/0306008].
[9] A. Cafarella, C. Coriano and T. N. Tomaras, JHEP **0506**, 065 (2005) [arXiv:hep-ph/0410358].
[10] M. Cavaglià, Int. J. Mod. Phys. A **18**, 1843 (2003) [arXiv:hep-ph/0210296];
G. Landsberg, J. Phys. G **32**, R337 (2006) [arXiv:hep-ph/0607297];
R. Emparan, *Black hole production at a TeV*, arXiv:hep-ph/0302226;
P. Kanti, Int. J. Mod. Phys. A **19**, 4899 (2004) [arXiv:hep-ph/0402168];
S. Hossenfelder, *What black holes can teach us*, arXiv:hep-ph/0412265;
V. Cardoso, E. Berti and M. Cavaglià, Class. Quant. Grav. **22**, L61 (2005) [arXiv:hep-ph/0505125].
[11] S. W. Hawking, Commun. Math. Phys. **43**, 199 (1975) [Erratum-ibid. **46**, 206 (1976)].
[12] E. J. Ahn and M. Cavaglià, Phys. Rev. D **73**, 042002 (2006) [arXiv:hep-ph/0511159];
The GROKE program can be downloaded at: http://www.phy.olemiss.edu/GR/groke.
[13] H. Yoshino and Y. Nambu, Phys. Rev. D **67**, 024009 (2003) [arXiv:gr-qc/0209003].
[14] H. Yoshino and V. S. Rychkov, Phys. Rev. D **71**, 104028 (2005) [arXiv:hep-th/0503171].
[15] T. Sjostrand, S. Mrenna and P. Skands, JHEP **0605**, 026 (2006) [arXiv:hep-ph/0603175];
See also: http://projects.hepforge.org/pythia6.
[16] S. J. Sciutto, *Air shower simulations with the AIRES system*, arXiv:astro-ph/9905185;
See also: http://www.fisica.unlp.edu.ar/auger/aires.
[17] V. Cardoso, M. Cavaglià and L. Gualtieri, JHEP **0602**, 021 (2006) [arXiv:hep-th/0512116];
V. Cardoso, M. Cavaglià and L. Gualtieri, Phys. Rev. Lett. **96**, 071301 (2006) [Erratum-ibid. **96**, 219902 (2006)] [arXiv:hep-th/0512002].
[18] G. Duffy, C. Harris, P. Kanti and E. Winstanley, JHEP **0509**, 049 (2005) [arXiv:hep-th/0507274];
M. Casals, P. Kanti and E. Winstanley, JHEP **0602**, 051 (2006) [arXiv:hep-th/0511163];

D. Ida, K. y. Oda and S. C. Park, Phys. Rev. D **71**, 124039 (2005) [arXiv:hep-th/0503052];
D. Ida, K. y. Oda and S. C. Park, Phys. Rev. D **73**, 124022 (2006) [arXiv:hep-th/0602188].
[19] D.N. Page, Phys. Rev. D **14**, 3260 (1976).
[20] R.C. Myers and M.J. Perry, Annals Phys. (N.Y.) **172**, 304 (1986).
[21] P. C. Aichelburg and R. U. Sexl, Gen. Rel. Grav. **2**, 303 (1971).
[22] S. C. Park and H. S. Song, J. Korean Phys. Soc. **43**, 30 (2003) [arXiv:hep-ph/0111069].